Coexistence of $\sqrt{3} \times \sqrt{3}$ and quasi-linear phases of sulfur adsorbed ($\Theta = 1/3$) on a gold (111) substrate

Sandra Carolina Gómez-Carrillo*[a] and Pablo Guillermo Bolcatto[ab]

Received 11th May 2010, Accepted 6th September 2010
DOI: 10.1039/c0cp00534g

We analyze with the aid of density functional theory and molecular dynamics simulations the adsorption of sulfur (S) on a Au(111) surface at different temperatures with a variety of geometries. We have found a new superficial phase in which sulfur atoms form a quasi-linear chain with energies very close to the expected $\sqrt{3} \times \sqrt{3}R30°$. The results suggest the coexistence of both configurations at $T < 300$ K. At high temperatures ($T > 300$ K) it was shown that the sulfur atoms have high mobility which allows their migration among different adsorption sites. At low temperatures, the mobility decreases and a thermal activation barrier of 25–30 meV can be estimated.

1. Introduction +

In the last few years, nanotechnology has opened new perspectives in all the fields of basic and applied sciences. The growth of gold nanoparticles has been used in many instances, supported on oxidic matrices such as ceria (CeO_2),[1,2] titania (TiO_2)[3,4] and other mixtures of oxides.[5,6] High growth control makes this noble metal very suitable for many heterogeneous catalytic gas–solid reactions.[7] Very high conversion rates ($\sim$100%) for the oxidation reaction of CO to CO_2 have been reached, eliminating in this way the residual (and contaminant) CO in the H_2 currents of fuel cells. Supported gold has also been used for the catalytic oxidation of hydrocarbons,[8–11] H_2O_2 formation using Au–Pd alloys,[12,13] H_2 production from methanol oxidation[14,15] and aldehyde hydrogenation.[16,17]

In catalysis science, the deactivation and regeneration processes that allows the extension of the useful lifetime of developed materials to be used as catalyzers was studied. Here, the presence of S in metal-based catalysts becomes undesirable due to the high reactivity of this element with metal degrades the efficiency of the catalyst. Thus, S is considered a poison and it is imperative to promote desulfurization reactions.[18,19]

On the other hand, in other fields of nanoscience, such as bioinspired devices[20] or molecular electronics,[21–26] S reactivity with metals is seen as an advantage. For example, in the case of the self-assembled structure formation of organothiol molecules,[27,28] the S terminal is an excellent connector between the metallic substrates and the adsorbed molecule or molecular wire.[29]

Therefore, either for its disadvantageous properties in catalysis or the desired ones for nanodevices or molecular electronics, the study of S adsorption onto gold is important both from the technological and basic points of view.

This is an active research area in which depending on the coverage and the temperature, a very rich variety of superficial S structures and adsorption properties are reported.[30–35] Restricting the analysis to Au(111) surfaces, coverages $\Theta \lesssim 1/3$ ML lead to regimes in which the adsorption is dominated by single S adatoms interacting with gold surfaces. The preferred adsorption site is an fcc hollow,[35,36] although for temperatures above $T = 550$ K migration to other sites is expected.[34] On the other side, for coverages greater than $\Theta \gtrsim 1/2$ ML, it is suggested that S atoms form more complex structures,[35] AuS compounds[32] or even superficial molecules S_n ($n = 2,\ldots,8$),[31,36] and in virtue of lattice parameters and atom–atom distances, each S will be localized at different adsorption sites (fcc hollow, hcp hollow, bridge, *etc.*).[31,36] Nevertheless, this scenario is still controversial and further studies are necessary.[37,38]

In an electrochemical environment, for $\Theta = 1/3$, scanning tunnelling microscopy (STM) images show a $\sqrt{3} \times \sqrt{3}R30°$ adlayer.[30,31] However, STM measurements performed on samples prepared by vaporization methods fail to show such structures. Only Low Energy Electron Diffraction (LEED) patterns compatible with a very unstable $\sqrt{3} \times \sqrt{3}R30°$ phase at room temperature are reported.[34,35] One possible reason could be the high mobility of S atoms but there is no direct evidence of this superficial motion.

This work explores the adsorption of S on the Au(111) surface with a coverage of $\Theta = 1/3$. Our results indicate a high mobility of S adatoms for temperatures above 300 K. Moreover, we have found two configurations in which the energies are compatible with a possible coexistence between them: the expected $\sqrt{3} \times \sqrt{3}$ and a novel quasi-linear phase in which the S atoms alternate fcc hollow and hcp hollow sites. The scheme of the paper is as follows. Section II introduces the numerical methods we used namely density functional theory (DFT). We perform simulations for several temperatures in which DFT is complemented with molecular dynamics (MD) calculations whose efficiency has been established in similar systems,[39–41] our results are fully discussed in section III. Section IV summarizes our conclusions.

[a] *Departamento de Física, Facultad de Ingeniería Química, Universidad Nacional del Litoral, Santiago del Estero 2829, S300AOM Santa Fe, Argentina. E-mail: scgomez@fiq.unl.edu.ar*
[b] *Facultad de Humanidades y Ciencias, Universidad Nacional del Litoral, Santa Fe, Argentina*

2. Theoretical and numerical methods

The calculations were done in the frame of the Local Density Approximation (LDA) to the DFT applied to systems with translational periodicity. We used the FIREBALL[42,43] code. In the theoretical approach, the electronic Hamiltonian stands for the valence electrons and the effect of the core electrons is incorporated *via* nonlocal norm-conserving pseudopotentials.[44] The basis-set is formed of (numerically) localized wave-functions which are strictly equal to zero beyond a proper cutoff radius, r_i (i = s, p, d). In this work we have selected $r_s = 4.3a_0$ and $r_p = 4.7a_0$ for S and $r_d = 4.1a_0$, $r_s = 4.6a_0$ and $r_p = 5.2a_0$ for gold, where a_0 is the Bohr radius. We have adopted a unit cell composed of four layers of gold, each one with six atoms, and two superficial S atoms so that the coverage is $\Theta = 1/3$ ML as is shown in Fig. 1. The cell has been replicated in the x–y superficial plane, and in the z-direction an empty space of the order of 200 Å (equivalent to ~83 layers) was added in order to simulate S superficial effects without interactions with the nearest cell along the z-direction. We did not take into account the herringbone reconstruction of the Au(111) surface because this is lost when a minimum S coating is added.[45,46] We have scanned several parameters like **k**-points, the number of iterations, tolerance, *etc*. and we estimated the numerical error for the *total* energy of the unit cell to be $\lesssim 10$ meV.

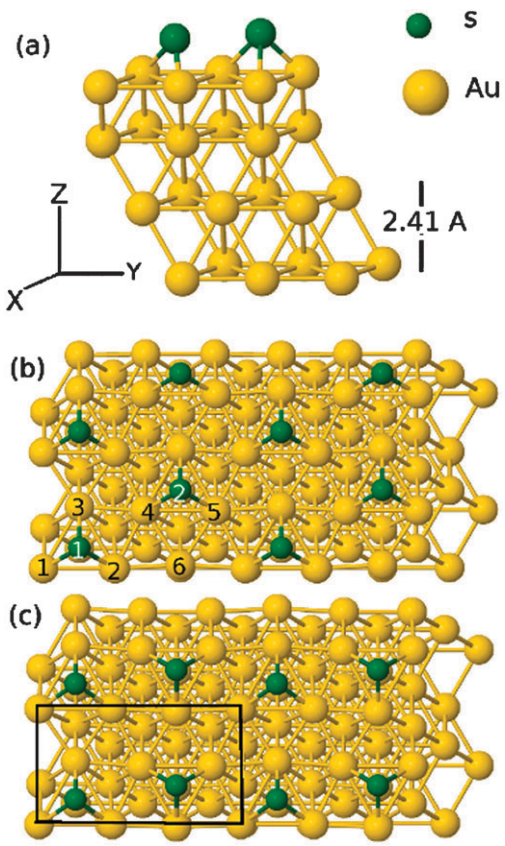

Fig. 1 (a) Unit cell used to simulate a coverage of $\Theta = 1/3$ ML. The cell is replicated in the x- and y-directions and a space equivalent to 83 layers was added in the z-direction in order to avoid spurious interactions between superficial S and bulk atoms. (b) and (c) top views of the $\sqrt{3} \times \sqrt{3}R30°$ and the quasi linear arrangements, respectively. The center of the Au1–Au2–Au3 (Au4–Au5–Au6) triangle is a fcc (hcp) site. The geometries are optimized at $T = 0$ K.

The calculation strategy had three steps: (i) Firstly, we looked for consistent configurations at a given temperature. The electronic calculations were complemented with classical MD. That is, at the beginning the atom velocities were assigned randomly following a Maxwell–Boltzmann distribution;[43] then, the atoms moved according to LDA forces and the velocities were rescaled in order to assure a constant kinetic energy (or temperature). The time step for the simulations was 0.2 fs and a maximum of 16 000 steps were calculated. The tolerance criteria for convergence is 10^{-4} eV atom^{-1} for the total energy and 10^{-2} eV Å^{-1} for the forces. In all cases only the innermost layer of gold is fixed and the three superficial ones plus the adatoms are free to move to optimize their energy. This DFT-MD technique has been successfully used in similar systems exhibiting dynamical fluctuations between two superficial phases.[39–41] (ii) Secondly, those configurations that reached the lowest total energy were recalculated at $T = 0$ K performing a minimization of energy following a dynamical quenching method.[47] (iii) Finally, in order to check the robustness of the results we performed cluster calculations using the final configuration of the unit cell. Here we changed the atomic basis set and different parameters for the exchange-correlation functional were tested. In this case, the calculations were done with the GAUSSIAN03 code.[48]

3. Results and discussion

3.1 $T \neq 0$ K calculations

Firstly we focused on the finite temperature behavior of the system. To do so, we explored different compatible geometric configurations at 800 K, 500 K, 300 K, 150 K and 1 K, respectively. Note that the selected time and number of steps did not attempt to reproduce either experimental cooling or a growth situation. The goal of this selection was to facilitate the system to reach low temperature phases corresponding to potential energy local minima which were not easily predicted from $T = 0$ K calculations.

We start with a fixed temperature of 800 K, this is a high value and stabilization of the system is not expected. Thermal desorption experiments starting from coverages above a monolayer reveal that at this temperature S begins to desorb, although not completely.[36] The reason why we started with this value was to promote disorder in the sample so that there were no preferred sites *a priori* for subsequent simulations. Fig. 2a shows the high mobility of S adatoms. They are able to migrate towards different sites without reaching a stable location (thin lines indicate the positions of S atoms for each step of the simulation). At the end of the simulation, S atoms were located near $\sqrt{3} \times \sqrt{3}$ hcp hollow sites. Together with this movement, the triangular Au(111) face was distorted not only in the x–y plane but also in z-direction as can be observed in Table 1. The values are the displacements with respect to the crystalline position after simulation. In particular for high temperatures, where the system does not reach stabilization,

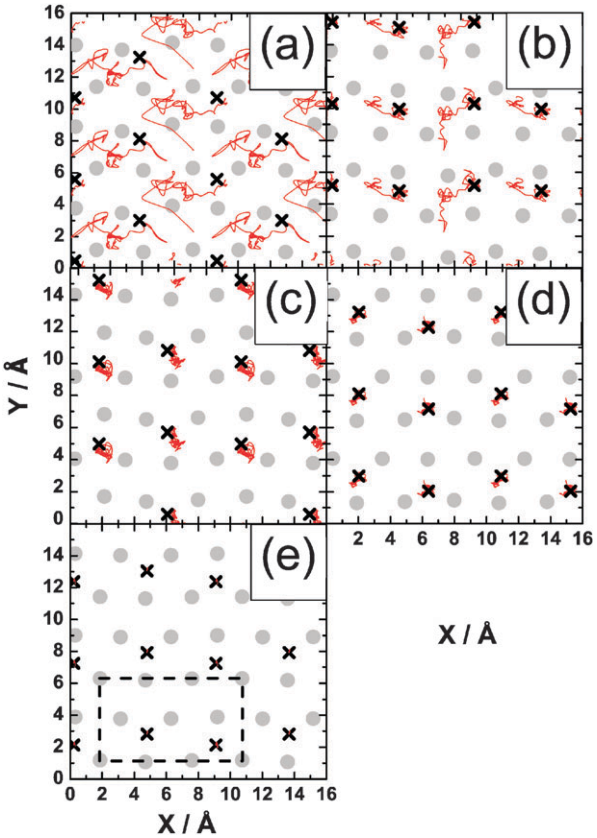

Fig. 2 Superficial phases (a) $T = 800$ K, (b) $T = 500$ K, (c) $T = 300$ K, (d) $T = 150$ K, (e) $T = 1$ K. The dashed rectangle in (e) shows the $\sqrt{3} \times \sqrt{3}$ unit cell. Thin red lines show the successive positions of S for each simulation step. Black crosses indicate the final location after simulation. Grey points are the final location of gold atoms of the outermost layer.

Table 1 Differences between (final) relaxed and crystalline z-positions of superficial gold atoms. The values are given in Å. As reference, the distance between (111) planes is 2.41 Å

	Δz			Δz		
	Au 1	Au 2	Au 3	Au 4	Au 5	Au 6
800 K	0.31	0.25	0.71	0.08	0.15	−0.13
500 K	0.12	−0.14	−0.21	0.05	0.28	−0.06
300 K	−0.38	0.07	−0.51	0.14	−0.54	0.55
150 K	−0.10	0.11	−0.15	−0.02	−0.03	0.23
1 K	−0.04	0.06	−0.07	−0.01	0.11	−0.08
0 K	—	—	—	—	—	—
Quasi-linear	0.07	0.07	−0.26	−0.01	−0.01	0.09
$\sqrt{3} \times \sqrt{3}$	−0.03	−0.03	−0.03	−0.03	−0.03	−0.03

these values are not physically significant but give us a quantitative idea about how distorted the substrate is when the calculations for the lower temperature starts.

The next step was to redefine the temperature. We chose 500 K and used the final geometry obtained for 800 K as the starting point for this second calculation. Here we also observed (Fig. 2b) an important mobility of S atoms. While each adatom follows a particular trajectory, both are able to jump towards nonequivalent hollow positions, even more than one time. This movement among different sites implies that a quasi-linear ordering occurs.

The third calculated temperature was 300 K and again, we started the calculation using the final geometry reached at 500 K. Less noticeable still than for 500 K, in this simulation at 300 K there is mobility of adatoms between bridge and hollow sites. For simulation times, S atoms oscillate 5–8 times between different bridge sites crossing hollow ones, but always inside the same triangle. When the adatom is positioned on a bridge site, it remains there for several steps with four-fold coordination, that is, just the limit before it jumps towards a non equivalent triangle.

The same calculation procedure is repeated for 150 K and 1 K. At 150 K, S atoms practically do not jump to different sites remaining near hollow locations (see Fig. 2d). For 1 K a quasi-linear phase is stabilized where S atoms occupy alternately fcc and hcp sites (see Fig. 2e). The evolution of the unit cell total energy for each step of DFT-MD simulation is presented in Fig. 3.

The vertical displacement of the first layer gold atoms with respect to the crystalline position is summarized in Table 1. Of particular interest is the case of 300 K, here the Au1–Au2–Au3 triangle is deformed so that two Au atoms go down and the third moves slightly up in relation to the initial z-position. On the other hand, the Au4–Au5–Au6 triangle is strongly distorted, with the Au6 atom displaced 0.55 Å outwards and the Au5 atom pushed down 0.54 Å. However, in spite of this clear corrugation, the situation is not compatible with a AuS superficial phase. The z-position of S is 1.88 Å (measured from the crystalline superficial gold plane) and the S–Au distances (Table 2) do not indicate the formation of a 1 : 1 superficial stoichiometric relation as was suggested in previous reports.[32,33] In our calculations, the equilibrium distance of the S–Au dimer is 2.23 Å. Nevertheless, further calculations with a major coverage and greater unit cell are necessary to explore the formation of gold sulfide and/or the occurrence of a "complex" phase as it was suggested in ref. 34 and 35.

The final phase corresponds to a local energy minimum although not necessarily an absolute minimum. For medium and low temperatures, the starting geometry is relevant to induce the stabilization of a particular phase. In order to check the coexistence between $\sqrt{3} \times \sqrt{3}$ and quasi-linear phases at

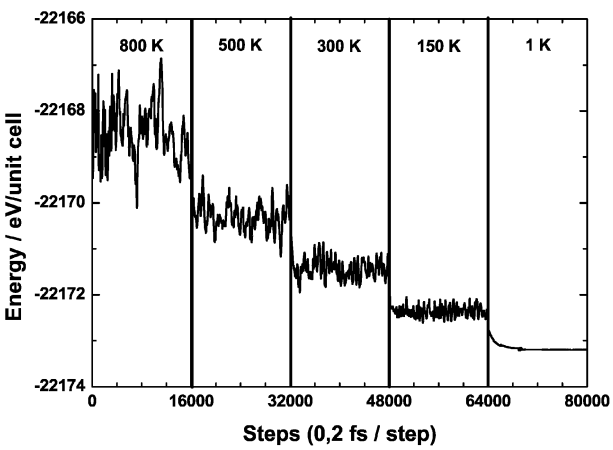

Fig. 3 Evolution of total energy for each simulation step.

Table 2 Distances between the S atoms and the first layer gold atoms. The values are given in Å

	300 K	1 K	0 K $\sqrt{3} \times \sqrt{3}$	0 K Quasi linear
d_{S1-Au1}	2.45	2.47	2.51	2.48
d_{S1-Au2}	2.93	2.54	2.51	2.48
d_{S1-Au3}	2.44	2.70	2.51	2.52
d_{S2-Au4}	2.49	2.44	2.51	2.51
d_{S2-Au5}	2.37	2.47	2.51	2.51
d_{S2-Au6}	2.62	2.32	2.51	2.49

room temperature, we have performed two complementary calculations starting from two different geometries than the ones used in the previous simulation at $T = 300$ K. After 5000 steps (5 fs step^{-1}) the S atoms are located in both $\sqrt{3} \times \sqrt{3}$ and quasi-linear phases. These results are presented in Fig. 4. Note that in spite of the different geometrical configurations, the total energy oscillates around almost the same mean value for the two calculations. Besides, it is remarkable that in these cases some jumps between non equivalent triangles were observed.

This behavior allowed us to do a rough, zero-order estimation of the activation barrier energy of 25–30 meV ($\gtrsim$300 K). This estimation is compatible with results arising from calculations done over the same system but with major coverages and greater unit cells.[49]

3.2 $T = 0$ K calculations

The appearance of the quasi-linear phase is somehow unexpected. Although very hard to stabilize in samples prepared in the gas phase,[35] the superficial ordering with $\sqrt{3} \times \sqrt{3}$ for $\Theta = 1/3$ symmetry seems to be the more favorable situation for the electrochemical environment.[30] To confirm the plausibility

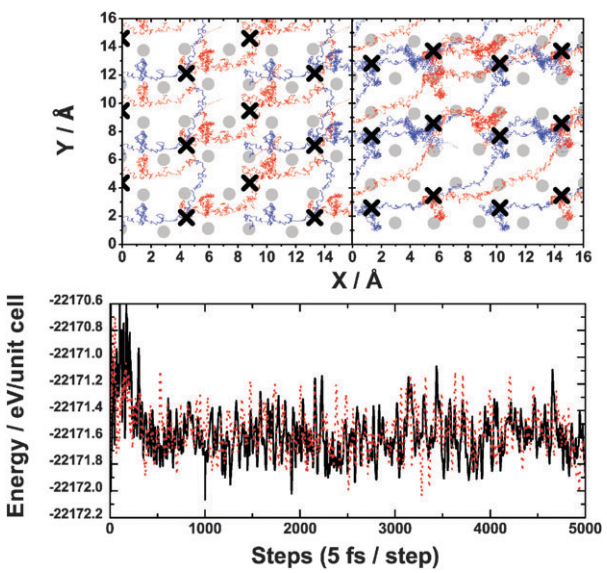

Fig. 4 Upper panel: evolution of positions for two different initial starting points. Red lines: S 1. Blue lines: S 2. The same conventions as Fig. 2. Lower panel: evolution of total unit cell energy. Red line corresponds to the left-upper panel calculation and the black line to the right-upper panel. The temperature of the simulations is $T = 300$ K and the time step is 5 fs step^{-1}.

Table 3 Total and binding energies for different configurations. The values correspond to the unit cell and are given in eV

$\Theta = 1/3$ $T = 0$ K	E_{total}	E_B^{S1-Au}	E_B^{S2-Au}	E_B^{S-S}
$\sqrt{3} \times \sqrt{3}$				
fcc-crystalline	−22172.6268	−4.972	−4.972	0.010
fcc-optimized	−22172.9998	−5.197	−5.203	−0.024
hcp-optimized	−22172.6349	−4.987	−4.980	0.010
quasi-linear	−22172.9753	−5.347 (fcc)	−5.032 (hcp)	−0.089

of the DFT-MD result, we have performed additional calculations at $T = 0$ K for different phases: (i) $\sqrt{3} \times \sqrt{3}$ with S atoms on fcc sites and gold atoms in crystalline positions, (ii) $\sqrt{3} \times \sqrt{3}$–fcc but allowing the system to relax towards an energy minimum following a dynamical quenching method,[47] (iii) the same as (ii) but with S atoms on hcp hollow sites, and (iv) the quasi linear structure, also allowing relaxation.

Table 3 resumes the relevant energies for each calculation. In addition to the total energy of the unit cell, we have calculated binding energies between S–Au and S–S defined as:

$$E_B^{S-Au} = E_{S-Au} - E_{Au} - E_S, \quad (1)$$

and

$$E_B^{S-S} = E_{total} - E_{S1-Au} - E_{S2-Au} - E_{Au} - 2E_S, \quad (2)$$

where E_{S-Au} (E_{Au}) is the total energy of a system identical to the final for each configuration but extracting one (two) S adatom. E_S is the energy of an isolated S atom.

Comparing the total energies of the unit cells, it is possible to verify that the optimized $\sqrt{3} \times \sqrt{3}$–fcc and quasi-linear structures are energetically more stable than the crystalline fcc and the relaxed hcp forms ($\Delta E \sim 370$ meV). This can be rationalized by analyzing the binding energies E_B^{S-Au} and E_B^{S-S}. In the more stable structures, the system gains energy compared to the crystalline form because the S atoms are more tightly bonded both to the surface and to the coadsorbed species.

As it is expected, in the quasi-linear phase the adsorption sites are not equivalent, the fcc hollow being the preferred place for the system to minimize its energy. However, as the S–S distance in the quasi-linear phase is lower than in the $\sqrt{3} \times \sqrt{3}$ phase (4.49 Å and 5.12 Å, respectively), the S–S bond is more important here (−89 meV against −24 meV). As reference, the equilibrium distance of the S–S dimer is 2.06 Å.

For the optimized $\sqrt{3} \times \sqrt{3}$–fcc phase, the gold superficial layer approaches the second layer (Table 1) and the S atoms are placed at the center of the fcc triangles (Table 2); while for the quasi-linear ordering, there is a slight corrugation which is reflected also in the S–Au distances. The reordering of superficial gold atoms leads to stabilization because the adatoms are able to be bind to the surface more tightly ($\sim$400 meV as it is estimated from Table 3)

On the other hand, it is noticeable that the difference between $\sqrt{3} \times \sqrt{3}$–fcc and the quasi-linear phases is in the order of the activation energy between fcc and hcp sites as it was estimated in the previous section ($\sim$25 meV), which could

Table 4 Total energies from cluster calculations. The values are in Hartree

	LDA	PBE
$\sqrt{3} \times \sqrt{3}R30°$	−3276.78026	−3272.10331
Quasi-linear	−3276.78012	−3272.10502

again account for a coexistence of these two phases at room temperature.

3.3 Gaussian calculations

In order to add new insights about the results of the previous sections, we recalculated the unit cell as a cluster changing the basis set and the exchange-correlation functional. For this purpose we used the GAUSSIAN03 code. In particular, we selected the LANLDZ atomic basis set[50] and the corresponding pseudopotential. We performed the calculations using LDA and the Perdew–Burke–Ernzernof (PBE) functional.[51] We used the optimized geometries resulting from FIREBALL results at $T = 0$ K (Fig. 1b–c). Cluster results also suggested the coexistence of both phases for this coverage.

Table 4 shows the resulting energy calculations. One can see that LDA gives very similar energies for both geometries, with the $\sqrt{3} \times \sqrt{3}R30°$ phase more stable only by 4 meV. However, when we change the exchange-correlation option the situation is inverse: the quasi-linear ordering minimizes the energy by 47 meV in relation to the $\sqrt{3} \times \sqrt{3}R30°$ phase.

4. Conclusions

In summary, we analyzed by means of LDA-DFT techniques the adsorption of S on a Au(111) surface for several temperatures which allowed us to explore a variety of geometries. For $T > 300$ K we have found that S atoms can migrate among different adsorption sites showing a high mobility. For lower temperatures the adatoms remain in nearly hollow sites and then we estimated a thermal activation barrier of 25–30 meV. In particular and of great interest, we found a new superficial phase in which S atoms form a quasi-linear chain with energies very near to the expected $\sqrt{3} \times \sqrt{3}R30°$ phase. Further calculations confirm this result suggesting the coexistence of both configurations at temperatures lower than 300 K.

Acknowledgements

We thank Guillermo Zampieri for fruitful discussions. The authors were supported by the Consejo Nacional de Investigaciones Científicas y Técnicas (CONICET). This work was performed thanks to Grant Nos 14248-128 of Fundación Antorchas and CAI + D PI-68-344 of Universidad Nacional del Litoral.

References

1 G. Yi, H. Yang, B. Li, H. Lin, K. ichi Tanaka and Y. Yuan, *Catal Today*, 2010, **1**, 1.
2 M. Manzoli, G. Avgouropoulos, T. Tabakova, J. Papavasiliou, T. Ioannides and F. Boccuzzi, *Catal. Today*, 2008, **138**, 239.
3 Y.-F. Yang, P. Sangeetha and Y.-W. Chen, *Int. J. Hydrogen Energy*, 2009, **34**, 8912.
4 Y. Denkwitz, B. Schumacher, G. Kucerov and R. J. Behm, *J. Catal.*, 2009, **267**, 78.
5 H. Wang, H. Zhu, Z. Qin, G. Wang, F. Liang and J. Wang, *Catal. Commun.*, 2008, **9**, 1487.
6 A. R. Vilchis-Nestor, M. Avalos-Borja, S. Gmez, J. A. Hernndez, A. Olivas and T. Zepeda, *Appl. Catal., B*, 2009, **90**, 64.
7 G. C. Bond, C. Louis and D. T. Thompson, *Catalysis by Gold*, Imperial College Press, London, vol. 6, 2006.
8 A. C. Gluhoi and B. E. Nieuwenhuys, *Catal. Today*, 2007, **119**, 305.
9 M. Gasior, B. Grzybowska, K. Samson, M. Ruszel and J. Haber, *Catal. Today*, 2004, **91–92**, 131.
10 D. Andreeva, P. Petrova, L. Ilieva, J. Sobczak and M. Abrashev, *Appl. Catal., B*, 2008, **77**, 364.
11 H. Dyrbeck and E. A. Blekkan, *Stud. Surf. Sci. Catal.*, 2007, **167**, 331.
12 G. Bernardotto, F. Menegazzo, F. Pinna, M. Signoretto, G. Cruciani and G. Strukul, *Appl. Catal., A*, 2009, **358**, 129.
13 F. Menegazzo, M. Signoretto, M. Manzoli, F. Boccuzzi, G. Cruciani, F. Pinna and G. Strukul, *J. Catal.*, 2009, **268**, 122.
14 F.-W. Chang, T.-C. Ou, L. S. Roselin, W.-S. Chen, S.-C. Lai and H.-M. Wu, *J. Mol. Catal. A: Chem.*, 2009, **313**, 55.
15 M. J. Lippits, R. R. H. B. Iwema and B. Nieuwenhuys, *Catal. Today*, 2009, **145**, 27.
16 C. Milone, M. Trapani and S. Galvagno, *Appl. Catal., A*, 2008, **337**, 163.
17 X. Li, B. Li, M. Cheng, Y. Du, X. Wang and P. Yang, *J. Mol. Catal. A: Chem.*, 2008, **284**, 1.
18 A. M. Venezia, V. L. Parola, G. Deganello, B. Pawelec and J. L. G. Fierro, *J. Catal.*, 2003, **215**, 317.
19 A. M. Venezia, R. Murania, G. Pantaleo, V. L. Parola, S. Scire and G. Deganello, *Appl. Catal., A*, 2009, **353**, 296.
20 A. Cossaro, *et al.*, *Langmuir*, 2006, **22**, 11193.
21 M. A. Reed, C. Zhou, C. J. Muller, T. P. Burgin and J. M. Tour, *Science*, 1997, **278**, 252.
22 C. Kergueris, J.-P Bourgoin, S. Palacin, D. Esteve, C. Urbina, M. Magoga and C. Joachim, *Phys. Rev. B: Condens. Matter Mater. Phys.*, 1999, **59**, 12505.
23 J. Ulrich, D. Esrail, W. Pontius, L. Venkataraman, D. Millar and L. H. Doerrer, *J. Phys. Chem.*, 2006, **110**, 2462.
24 X. Li, J. He, J. Hihath, B. Xu, S. M. Lindsay and N. Tao, *J. Am. Chem. Soc.*, 2006, **128**, 2135.
25 C. Li, I. Pobelov, T. Wandlowski, A. Bagrets, A. Arnold and F. Evers, *J. Am. Chem. Soc.*, 2008, **130**, 318.
26 M. Kiguchi, O. Tal, S. Wohlthat, F. Pauly, M. Krieger, D. Djukic, J. C. Cuevas and J. M. van Ruitenbeek, *Phys. Rev. Lett.*, 2008, **101**, 046801.
27 F. Schreiber, *Prog. Surf. Sci.*, 2000, **65**, 151.
28 B. D. Gates, Q. Xu, M. Stewart, D. Ryan, C. G. Wilson and G. M. Whitesides, *Chem. Rev.*, 2005, **105**, 1171.
29 C. Love, L. A. Estroff, J. K. Kriebel, R. G. Nuzzo and G. M. Whitesides, *Chem. Rev.*, 2005, **105**, 1103.
30 C. Vericat, M. E. Vela, G. Andreasen, R. C. Salvarezza, L. Vázquez and J. A. Martin-Gago, *Langmuir*, 2001, **17**, 4919.
31 C. Vericat, M. E. Vela, J. Gago and R. C. Salvarezza, *Electrochim. Acta*, 2004, **49**, 3643.
32 M. M. Biener, J. Biener and C. M. Friend, *Langmuir*, 2005, **21**, 1668.
33 S. Y. Quek, M. M. Biener, J. Biener, J. Bhattacharjee, C. M. Friend, U. V. Waghmare and E. Kaxiras, *J. Phys. Chem. B*, 2006, **110**, 15663.
34 M. M. Biener, J. Biener and C. M. Friend, *Surf. Sci.*, 2007, **601**, 1659.
35 M. Yu, H. Ascolani, G. Zampieri, D. P. Woodruff, C. J. Satterley, R. G. Jones and V. R. Dhanak, *J. Phys. Chem. C*, 2007, **111**, 10904.
36 J. A. Rodriguez, J. Dvorak, T. Jirsak, G. Liu, J. Hrbek, Y. Aray and C. Gonzalez, *J. Am. Chem. Soc.*, 2003, **125**, 276.
37 P. G. Lustemberg, C. Vericat, G. A. Benitez, M. E. Vela, N. Tognalli, A. Fainstein, M. L. Martiarena and R. C. Salvarezza, *J. Phys. Chem. C*, 2008, **112**, 11394.
38 P. N. Abufager, P. G. Lustemberg, C. Crespos and H. F. Busnengo, *Langmuir*, 2008, **24**, 14022.
39 J. Avila, A. Mascaraque, E. G. Michel, M. C. Asensio, G. LeLay, J. Ortega, R. Pérez and F. Flores, *Phys. Rev. Lett.*, 1999, **82**, 442.

40 D. Farías, W. Kaminski, J. Lobo, J. Ortega, E. Hulpke, R. Pérez, F. Flores and E. G. Michel, *Phys. Rev. Lett*., 2003, **91**, 016103.
41 C. González, F. Flores and J. Ortega, *Phys. Rev. Lett*., 2006, **96**, 136101.
42 O. F. Sankey and D. J. Niklewski, *Phys. Rev. B: Condens.Matter*, 1989, **40**, 3979.
43 A. A. Demkov, J. Ortega, O. F. Sankey and M. P. Grumbach, *Phys. Rev. B: Condens. Matter*, 1995, **52**, 1618.
44 D. R. Hamann, *Phys. Rev. B: Condens. Matter*, 1989, **40**, 2980.
45 C. Wll, S. Chiang, R. J. Wilson and P. H. Lippel, *Phys. Rev. B: Condens. Matter*, 1989, **39**, 7988.
46 J. V. Barth, R. Schuster, R. J. Behm and G. Ertl, *Surf. Sci*., 1996, **348**, 280.
47 O. F. Sankey, A. A. Demkov, W. Windl, J. H. Firsch, J. P. Lewis and M. Fuente-Cabrera, *Int. J. Quantum Chem*., 1998, **69**, 327.
48 M. J. Frisch, G. W. Trucks, H. B. Schlegel, G. E. Scuseria, M. A. Robb, J. R. Cheeseman, J. A. Montgomery, Jr., T. Vreven, K. N. Kudin, J. C. Burant, J. M. Millam, S. S. Iyengar, J. Tomasi, V. Barone, B. Mennucci, M. Cossi, G. Scalmani, N. Rega, G. A. Petersson, H. Nakatsuji, M. Hada, M. Ehara, K. Toyota, R. Fukuda, J. Hasegawa, M. Ishida, T. Nakajima, Y. Honda, O. Kitao, H. Nakai, M. Klene, X. Li, J. E. Knox, H. P. Hratchian, J. B. Cross, V. Bakken, C. Adamo, J. Jaramillo, R. Gomperts, R. E. Stratmann, O. Yazyev, A. J. Austin, R. Cammi, C. Pomelli, J. Ochterski, P. Y. Ayala, K. Morokuma, G. A. Voth, P. Salvador, J. J. Dannenberg, V. G. Zakrzewski, S. Dapprich, A. D. Daniels, M. C. Strain, O. Farkas, D. K. Malick, A. D. Rabuck, K. Raghavachari, J. B. Foresman, J. V. Ortiz, Q. Cui, A. G. Baboul, S. Clifford, J. Cioslowski, B. B. Stefanov, G. Liu, A. Liashenko, P. Piskorz, I. Komaromi, R. L. Martin, D. J. Fox, T. Keith, M. A. Al-Laham, C. Y. Peng, A. Nanayakkara, M. Challacombe, P. M. W. Gill, B. G. Johnson, W. Chen, M. W. Wong, C. Gonzalez and J. A. Pople, *GAUSSIAN 03 (Revision D.01)*, Gaussian, Inc., Wallingford, CT, 2004.
49 S. C. Gómez-Carrillo and P. G. Bolcatto, in preparation.
50 P. J. Hay and W. R. Wadt, *J. Chem. Phys*., 1985, **82**, 270.
51 J. P. Perdew, K. Burke and M. Ernzernof, *Phys. Rev. Lett*., 1996, **77**, 3865.

